

Neutron capture cross sections of  $^{93}\text{Nb}$ K. S. Krane *Department of Physics, Oregon State University, Corvallis, Oregon 97331, USA*

(Received 17 May 2019; published 17 September 2019)

The radiative cross sections for neutron capture by  $^{93}\text{Nb}$  to form the ground state of  $^{94}\text{Nb}$  have been determined to be  $\sigma_g = 0.18(8)$  b and  $I_g = 5.2(8)$  b by an activation study of the  $\gamma$  rays emitted in the decays of  $^{94}\text{Nb}^{g,m}$ . This determination required the correction of the total production of the ground state in neutron capture for the production through the decay of the isomer, in the process of which the cross sections of the isomer were determined to be  $\sigma_m = 0.78(9)$  b and  $I_m = 5.6(7)$  b. The values of the cross sections are discussed on the basis of the resonance structure of  $^{94}\text{Nb}$  and also in comparison with the similar cases of neutron capture by  $^{59}\text{Co}$  and  $^{165}\text{Ho}$ . Also reported are new determinations of the energies and intensities of the  $\gamma$  rays emitted in the decays of  $^{94}\text{Nb}^{g,m}$  and  $^{92}\text{Nb}^m$ .

DOI: [10.1103/PhysRevC.100.034613](https://doi.org/10.1103/PhysRevC.100.034613)

## I. INTRODUCTION

Neutron capture by  $^{93}\text{Nb}$  (the only stable isotope of Nb) with  $J^\pi = 9/2^+$  results in population of the 20 000-yr ground state ( $J^\pi = 6^+$ ) and the 6-min 41-keV isomer ( $J^\pi = 3^+$ ) in  $^{94}\text{Nb}$ . Both product states can be formed by  $s$ -wave or  $p$ -wave neutron capture leading to resonances of spins between 3 and 6, followed by single or double dipole  $\gamma$  emission. Both states decay by  $\beta$  emission to excited states in  $^{94}\text{Mo}$ , hence the neutron capture cross sections should be measurable by the activation technique through observation of the  $\gamma$  rays in the daughter. However, to date the only reported measurements are the cross section for direct production of the isomer [1–5] and that for the combined production of the ground state including indirect production through the decay of the isomer [6]. There has been no value reported for the direct production of the ground state in the absence of the decay of the isomer.

The present paper describes a measurement of the isomeric and combined thermal cross sections of Nb by observing their radioactive decays. From knowledge of the production of the isomer, it is then possible to remove its contribution to the combined production leading to the ground state and so deduce the cross section for direct production of the ground state. Also reported here are new determinations of the energies of the  $\gamma$  rays emitted in the  $^{94}\text{Nb}^{g,m}$  decays and also in the decays of 10-d  $^{92}\text{Nb}^m$  which was present in the radioactive samples as a result of the  $(n, 2n)$  reaction.

## II. EXPERIMENTAL DETAILS

The samples for these experiments consisted of Nb metal foil of thickness 0.05 mm. Samples were irradiated at various sites in the Oregon State University TRIGA reactor: the periphery of the core with thermal and epithermal fluxes of  $\phi_{\text{th}} = 4.4 \times 10^{12}$  neutrons  $\text{cm}^{-2} \text{s}^{-1}$  and  $\phi_{\text{epi}} = 3.5 \times 10^{11}$  neutrons  $\text{cm}^{-2} \text{s}^{-1}$ ; a Cd-lined site in the central core ( $\phi_{\text{th}} \approx 0$  and  $\phi_{\text{epi}} = 1.1 \times 10^{12}$  neutrons  $\text{cm}^{-2} \text{s}^{-1}$ );

thermal column ( $8.0 \times 10^{10}$  and  $2.0 \times 10^8$  neutrons  $\text{cm}^{-2} \text{s}^{-1}$ ); and a fast pneumatic transfer facility or rabbit ( $7.1 \times 10^{12}$  and  $3.4 \times 10^{11}$  neutrons  $\text{cm}^{-2} \text{s}^{-1}$ ). For the decays of the long-lived ground state, sample masses ranged from 118 mg in the core sites to 277 mg in the thermal column. For the short-lived isomer decays studied through production in the rabbit, sample masses were typically 5–10 mg, and experiments were done by irradiating both bare and Cd-wrapped samples to separate the thermal and epithermal contributions to the activation. The results for the thermal cross sections presented in this paper are based on data from four samples (one thermal column, one outer core, two rabbit), and the resonance integrals are derived from data on five samples (two Cd-lined core site, three Cd-wrapped rabbit).

End-of-bombardment (EOB) activities produced to study the ground-state decay ranged from 1 Bq (corresponding to a count rate of the order of 500 per day in the analysis lines) in the thermal column to 20–30 Bq (5000 per day) in the core irradiations. The rabbit samples produced to study the decay of the isomer typically had EOB activities in the range of 10–50 MBq; counting of the samples commenced within minutes of EOB and produced several thousand counts per minute in the analysis line.

The  $\gamma$  rays following the  $^{94}\text{Nb}$   $\beta$  decays were observed with Ge detectors (resolution 1.8–2.0 keV and intrinsic efficiency 40% relative to NaI at 1332 keV) coupled to a digital signal processor-based data acquisition system. Peaks in the spectrum were well isolated, and as a result the ORTEC GAMMAVISION software [7], which sums counts above a linear background, could easily be used for the determination of their intensities in the cross-section measurements. For the spectroscopic measurements of the  $\gamma$ -ray energies and intensities, the peaks were fitted to Gaussian shapes with tails using the SAMPO software [8]. Energy and efficiency calibrations were done using sources of  $^{133}\text{Ba}$ ,  $^{152}\text{Eu}$ , and  $^{207}\text{Bi}$ . Additional internal calibration was provided through the decay of  $^{182}\text{Ta}$ , which was produced by activation of a 40-ppm Ta impurity in

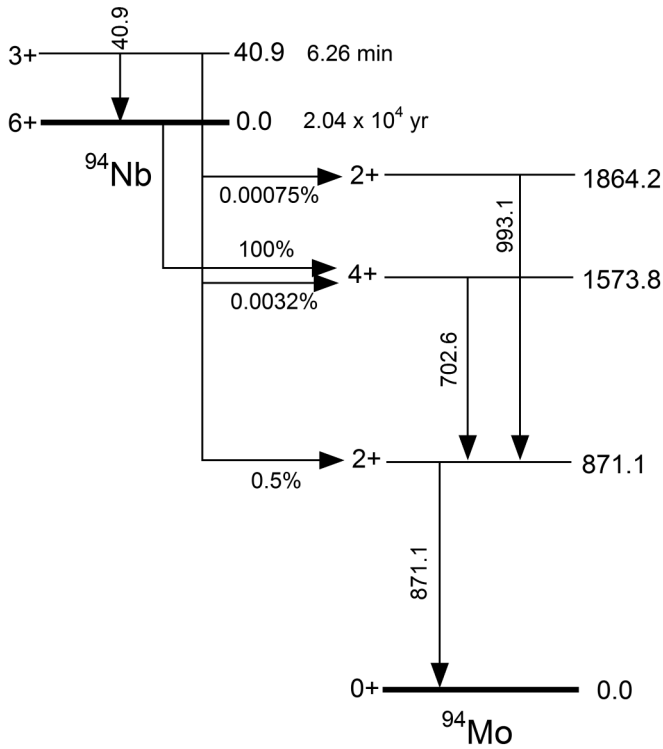


FIG. 1. Decays of  $^{94}\text{Nb}^{g,m}$  to levels of  $^{94}\text{Mo}$ . Level and  $\gamma$ -ray energies are given in keV.

the samples (Ta being just below Nb in the periodic table and thus very similar chemically).

The EOB activities  $a$  produced following irradiation of  $N$  target atoms for a time  $t_i$  depend on the cross sections according to

$$a = N(\sigma\phi_{\text{th}} + I\phi_{\text{epi}})(1 - e^{-\lambda t_i}), \quad (1)$$

where  $\sigma$  is the effective thermal cross section and  $I$  is the effective resonance integral. Self-absorption of thermal and epithermal neutrons is estimated to be minimal, well within the uncertainty of the deduced cross sections imposed by the neutron flux. All Nb irradiations were accompanied by Au, Co, and Zr flux monitors.

Figure 1 shows the basics of the decays of  $^{94}\text{Nb}^{g,m}$ ; details were taken from the latest compilation of the Nuclear Data Sheets (NDS) [9]. The  $^{94}\text{Nb}^m$  decays to  $^{94}\text{Nb}^g$  through an  $M3$  isomeric transition of energy 40.9 keV in 99.5% of the decays; unfortunately this transition is both highly converted and strongly absorbed, and the determination of the effective Ge detector efficiency in this energy region cannot be done with sufficient precision. Thus it is necessary to employ the 871.1-keV transition that follows the 0.50(6)%  $\beta$  decay as a monitor of the isomeric state decay, which imposes a fairly large uncertainty (12%) on the final conclusions. The NDS value for the half-life of  $^{94}\text{Nb}^g$  would impose a similarly large uncertainty (8%) on conclusions based on its decay, but a more recently determined value of the half-life of  $2.04(4) \times 10^4$  yr [10] reduces its contribution to the overall uncertainty to 2%.

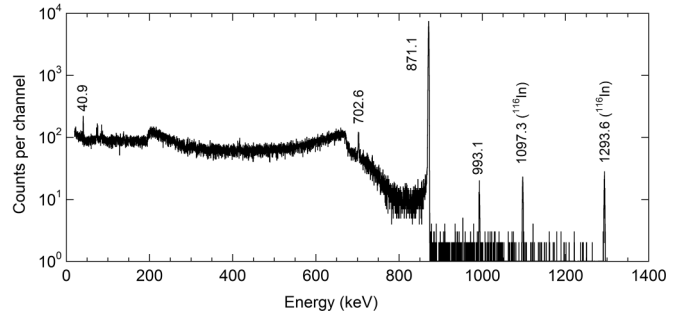


FIG. 2. Spectrum of  $\gamma$  rays from the decay of  $^{94}\text{Nb}^m$  taken about 10 min following irradiation.

### III. RESULTS

Figure 2 shows a spectrum of  $\gamma$  rays from the decay of  $^{94}\text{Nb}^m$  accumulated for about 10 min after irradiation in the rabbit, and Fig. 3 shows the spectrum from the decay of a  $^{94}\text{Nb}^g$  sample. In addition to the  $^{182}\text{Ta}$  impurity, this spectrum shows characteristic lines from the decay of 10-d  $^{92}\text{Nb}^m$ , presumably formed from the  $(n, 2n)$  reaction. Normally this reaction would not produce such an easily observable activity, due to its small cross section (in the millibarn range) and the relatively small flux of fast neutrons, but the small decay rate associated with the long half-life of  $^{94}\text{Nb}^g$  allows the  $^{92}\text{Nb}^m$  to compete successfully. Fortunately, neither the  $^{182}\text{Ta}$  nor the  $^{92}\text{Nb}$  lines lie close to the two prominent  $^{94}\text{Nb}$  lines and so there is no interference of the other activities with the measurement.

The dominant contribution to the uncertainty in the  $^{94}\text{Nb}^m$  cross sections results from the 12% uncertainty in the  $\beta$  decay branching. The neutron flux contributes 3% to the uncertainty, and all other factors (sample mass, half-life, detector efficiency, and counting statistics) contribute no more than 1% each. The resulting cross sections for the formation of  $^{94}\text{Nb}^m$  were determined to be

$$\sigma_m = 0.78(9) \text{ b},$$

$$I_m = 5.6(7) \text{ b}.$$

Were it not for the branching uncertainty, the uncertainties in  $\sigma_m$  and  $I_m$  would be reduced to respectively 0.03 and 0.2 b.

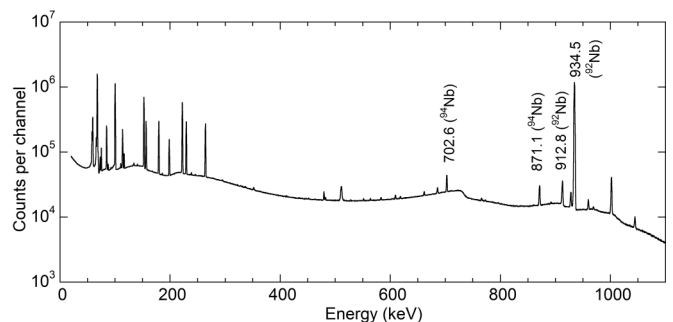


FIG. 3. Spectrum of  $\gamma$  rays from the decay of  $^{94}\text{Nb}^g$ . Most of the unmarked peaks are due to the decay of the  $^{182}\text{Ta}$  impurity.

TABLE I. Gamma rays emitted in the decays of  $^{94}\text{Nb}^{g,m}$  and  $^{92}\text{Nb}^m$ .

| Decay              | Previous work <sup>a</sup> |                      |                                  | Present work |          |                     |
|--------------------|----------------------------|----------------------|----------------------------------|--------------|----------|---------------------|
|                    | $E$ (keV)                  | $I$                  | Initial state (keV) <sup>b</sup> | $E$ (keV)    | $I$      | Initial state (keV) |
| $^{94}\text{Nb}^m$ | 702                        | 0.63(4)              | 1573.76(4)                       |              | 0.78(8)  |                     |
|                    | 871                        | 100                  | 871.098(16)                      |              | 100(1)   |                     |
|                    | 993                        | 0.15(2)              | 1864.31(5)                       | 993.13(6)    | 0.20(2)  | 1864.22(6)          |
| $^{94}\text{Nb}^g$ | 702.622(19)                | 100                  | 1573.76(4)                       | 702.649(10)  | 99.6(5)  | 1573.751(14)        |
|                    | 871.091(18)                | 100                  | 871.098(16)                      | 871.095(10)  | 100.0(5) | 871.099(10)         |
| $^{92}\text{Nb}^m$ | 912.6(2)                   | 1.8(1) <sup>b</sup>  | 1847.27(4)                       | 912.803(15)  | 1.79(2)  | 1847.316(9)         |
|                    | 934.3(1)                   | 100 <sup>b</sup>     | 934.51(4)                        | 934.510(10)  | 100(1)   | 934.515(10)         |
|                    | 1847.5(3)                  | 0.86(4) <sup>b</sup> | 1847.27(4)                       | 1847.294(10) | 0.910(9) | 1847.316(9)         |

<sup>a</sup> $^{94}\text{Nb}^m$ : Hayashibe *et al.* [11];  $^{94}\text{Nb}^g$ : Helmer *et al.* [12];  $^{92}\text{Nb}^m$ : Berman and Baglan [13].

<sup>b</sup>From NDS compilations for  $A = 94$  [9] and  $A = 92$  [14].

Using these values of the cross sections for the direct production of  $^{94}\text{Nb}^m$ , the resulting number of  $^{94}\text{Nb}^g$  formed in the decay of the isomer can be calculated and subtracted from the total number of  $^{94}\text{Nb}^g$  deduced from the decay activity. Typically the number of  $^{94}\text{Nb}^g$  produced through the decay of the isomer was about 1/2 of the total number in the resonance integral experiments on the Cd-lined irradiation site and about 2/3–3/4 of the total number in the thermal cross section experiments in the core and thermal column sites, so the subtraction had a large effect. As a result, the effect of the uncertainty in the cross sections of the isomer was considerably magnified in the determination of the ground-state thermal cross section and slightly less for the resonance integral. The uncertainty in the isomer cross section (resulting from the uncertainty in the  $\beta$  decay branching) produced an uncertainty of 0.08 b in the thermal cross section of the ground state. Counting statistics and the neutron flux each contributed about 0.02 b, and the remaining factors (half-life, sample mass, detector efficiency, and  $\gamma$ -ray branching) all contributed less than 0.01 b to the net uncertainty.

Prior to the subtraction, the total value of the thermal cross section for production of the ground state (including indirect production through the isomer) was determined to be 1.06(4) b, in excellent agreement with the previous consensus value of 1.15(5) b [6]. After the subtraction, the value of the thermal cross section determined in the core irradiation was 0.21(8) b and that from the thermal column irradiation was 0.14(8) b. A similar subtraction method was used to obtain the ground-state resonance integral from the measurements on the Cd-lined irradiation site. The final values for the ground-state cross sections are

$$\sigma_g = 0.18(8) \text{ b},$$

$$I_g = 5.2(8) \text{ b}.$$

Counting the Nb samples both in isolation (with the internal  $^{182}\text{Ta}$  for calibration) as well as with external calibration sources of  $^{152}\text{Eu}$  and  $^{207}\text{Bi}$  enabled a new determination of the energies and intensities of the  $\gamma$  rays emitted by  $^{94}\text{Nb}^{g,m}$

and  $^{92}\text{Nb}^m$ . The identity of the  $^{92}\text{Nb}^m$  impurity was verified by a determination of its half-life based on following the decay of the 934-keV line (normalized by the lines from a simultaneously counted  $^{152}\text{Eu}$  source to guard against variations in the dead time of the counting system) over 4 weeks, which yielded  $t_{1/2} = 10.07(2)$  d, in agreement with the NDS value of 10.15(2) d.

Table I summarizes the  $\gamma$ -ray energies and intensities deduced from the present spectra, along with the energy levels in the  $^{94}\text{Mo}$  and  $^{92}\text{Zr}$  daughters. The rabbit experiments with the 6-min  $^{94}\text{Nb}^m$  did not include calibration sources, so the energy of the 993.1-keV line was determined in comparison with that of the 871.1-keV line and the 1097.3- and 1293.6-keV lines from the weak  $^{116}\text{In}$  activity (due to activation of an 80-ppm  $^{115}\text{In}$  impurity). Overall the agreement between the previous results [9,11–14] and the generally more precise current results is very good.

#### IV. DISCUSSION

A previous measurement of the thermal cross section to form  $^{94}\text{Nb}^m$  by activation by De Corte and Simonits [1] yielded the value  $\sigma_m = 0.86(10)$  b, in agreement with the present value while also suffering from the 12% uncertainty imposed by the branching ratio of the isomer decay. The resonance integral to form the isomer was previously measured by Ryves [2] and by Sage and Furr [3] yielding respective values 6.2(14) b and 6.6(20) b, in agreement with the present result but with larger uncertainties. The dimensionless ratio  $Q_m = I_m/\sigma_m$  for the isomer (which is independent of the branching ratio) was measured to be 7.35(20) by Simonits *et al.* [4] and 7.28(11) by Farina Arboc c  *et al.* [5], in agreement with the value 7.18(22) deduced from the present data.

Capture of  $s$ -wave neutrons by the  $9/2^+$   $^{93}\text{Nb}$  ground state leads to  $4^+$  and  $5^+$  resonances, which can then respectively decay directly to the  $3^+$  and  $6^+$  states in  $^{94}\text{Nb}$  through magnetic dipole ( $M1$ ) transitions. Capture of  $p$ -wave neutrons leads to  $3^-$ ,  $4^-$ ,  $5^-$ , and  $6^-$  resonances, which can decay to the  $^{94}\text{Nb}$  ground and isomeric states through electric dipole ( $E1$ ) transitions. Experimental data as well as optical model calculations [15] show a minimum in the  $s$ -wave strength and

a maximum in the  $p$ -wave strength in the mass region  $A = 90$ – $100$ . Moreover, the probability for  $E1$  emission dominates over that for  $M1$  emission by 1–2 orders of magnitude. Thus it is expected that the  $p$ -wave resonances will be significant contributors to the  $^{93}\text{Nb}(n,\gamma)$  cross sections.

Kompe [16] has determined the  $p$ -wave strength for Nb from  $(n,\gamma)$  cross section measurements in the energy region 10–100 keV and has similarly concluded that the  $p$ -wave contribution dominates the cross section. In the energy region 10 eV–10 keV, the resonances all contribute to the value of the resonance integral, and with many  $p$ -wave resonances of all possible spins (3–6) present (the tabulation of Mughabghab [6] shows 200 resonances of various spins), there should be no significant distinction between the formation of the  $6^+$  ground state and the  $3^+$  isomer in  $^{94}\text{Nb}$ . Indeed, the measured resonance integrals for the two states are virtually identical, respectively 5.2(8) and 5.6(7) b.

However, the situation is quite different for the thermal cross sections. The lowest neutron resonance occurs at 36 eV, and the low-lying resonances are narrow and can be analyzed using the Breit-Wigner shape. In this analysis, when the resonances are far removed from the thermal region, the cross section in the thermal region shows the usual  $1/v$  dependence on the velocity of the neutron, and the contribution of each resonance to the thermal cross section is approximately proportional to the dimensionless parameter  $\Gamma_n\Gamma_\gamma/E_R^2$ , where  $\Gamma_n$  is the neutron contribution to the resonance width,  $\Gamma_\gamma$  is the partial width for  $\gamma$  emission, and  $E_R$  is the resonance energy. (This approximation assumes that  $E_R$  is much greater than both the neutron kinetic energy and the total width, which is valid for the Nb resonances.) The  $\gamma$ -ray partial width is roughly constant over the lower resonances, while on the average the neutron width increases approximately like  $E_R^{1/2}$ . The value of  $\Gamma_n\Gamma_\gamma/E_R^2$  thus drops off rapidly with increasing  $E_R$ , and so the thermal cross section is generally determined by only a few lower-energy resonances.

The resonance energies and partial widths have been tabulated by Mughabghab [6], and values from more recent measurements may be found in Drindak *et al.* [17] and Wang *et al.* [18]. There are seven prominent resonances below 300 eV. Three of these are  $s$ -wave and four are  $p$ -wave. The four  $p$ -wave resonances (with spins 3, 4, 4, and 5) contribute mostly to forming the  $3^+$  isomeric state. Of the three  $s$ -wave resonances (spins 4, 5, and 5), one with spin 5 has an anomalously large neutron width (an order of magnitude larger than all other low-lying resonances), which leads to the prediction that its contribution should dominate in thermal capture and thus that the  $6^+$  ground state would preferentially be formed, in contradiction to the measured values of the thermal cross sections. A direct measurement by Kennett *et al.* [19] of the  $M1$  strengths of primary radiations following thermal capture showed that population of the isomer dominates over the ground state by an order of magnitude, which replicates the behavior of the thermal cross sections. From a study of resonance neutron capture by  $^{93}\text{Nb}$ , Chrien *et al.* [20] concluded that there is an enhancement of the  $E1$  over the  $M1$  strengths, which would tend to magnify the  $p$ -wave contribution to the cross section and thus in turn

favor the formation of the  $3^+$  isomer. Perhaps a similar effect contributes to the relative magnitudes of the thermal cross sections.

There are two other nuclides for which the spins of the isomer and ground state produced in radiative neutron capture are equidistant above and below the spin of the stable target, as is the case for  $^{93}\text{Nb}$ . Capture by  $^{59}\text{Co}$  ( $7/2^-$ ) leads to the 10-min  $2^+$  isomer at 59 keV and the 5-yr  $5^+$  ground state in  $^{60}\text{Co}$ . There is a peak in the  $s$ -wave cross section near  $A = 60$  [15].  $s$ -wave capture leads to  $3^-$  and  $4^-$  resonances, which can decay to the respective states in  $^{60}\text{Co}$  by a single  $E1$  transition. In this case the ratio of the low-spin to high-spin thermal cross sections is 1.2, so the formation of the low spin is only slightly favored, in contrast to the case for  $^{93}\text{Nb}$ . The many intermediate energy resonances result in a more equal ratio of the resonance integrals of 1.1, in analogy with  $^{93}\text{Nb}$ . The second similar case involves capture by  $^{165}\text{Ho}$  ( $7/2^-$ ) leading to the 1200-yr  $7^-$  isomer at 6 keV and the 27-h  $0^-$  ground state in  $^{166}\text{Ho}$ . A peak in the  $s$ -wave cross section also exists near  $A = 160$ , and there are many  $3^-$  and  $4^-$   $s$ -wave resonances in  $^{166}\text{Ho}$ . However, in this case formation of the high-spin isomer is strongly suppressed: the ratio of the thermal cross sections is about 20 and that of the resonance integrals is about the same. In this case a cascade of at least three dipole  $\gamma$  rays is necessary to reach either the isomer or the ground state from the  $s$ -wave resonances. The probability for either cascade reflects the spin dependence of the nuclear level density, which declines rapidly for the higher spins. [21] Thus the  $\gamma$ -ray cascade leading from the  $4^-$  resonance to the  $7^-$  state is less probable than the cascade from the  $3^-$  resonance to the  $0^-$  state, resulting in the smaller cross section for the former process.

An independent determination of the thermal cross section of the  $^{94}\text{Nb}^m$  isomeric state comes from a study of the primary and secondary  $\gamma$  rays emitted following neutron capture [22]. The result,  $\sigma_m = 0.783(13)$  b, agrees with the present result but is more precise because it does not depend on the  $\beta$  decay branching with its large relative uncertainty. An alternative way to analyze the present results is then to assume the value of the isomeric cross section determined from the prompt  $\gamma$  rays and then deduce the corresponding value of the  $\beta$  decay branching that would produce that value (and its uncertainty) in the activation experiment. The resulting  $\beta$  intensity for the decay of the isomer is 0.529(17)%, where the uncertainty includes contributions from the thermal cross section (0.007%), the sample mass (0.010%), neutron flux (0.010%), detector efficiency (0.005%), and resonance integral value (0.005%). The corresponding value of the resonance integral, based on the present results and using the new value of the  $\beta$  intensity, is  $I_m = 5.58(21)$  b. Again using the cross sections of the isomer to determine how many of the ground-state decays occurred through direct production and how many due to the decay of the isomer, the ground-state cross sections are deduced to be  $\sigma_g = 0.21(6)$  b and  $I_g = 5.55(41)$  b. These values overlap with the values determined from the activation data alone but have slightly smaller uncertainties. As in the case of the activation values, the large relative uncertainty of the thermal cross section is a result of the

subtraction of the isomer production, which magnifies the relative uncertainties.

## V. CONCLUSIONS

After correcting for the production of the ground state by the decay of the isomer, the cross sections for the  $^{93}\text{Nb}(n,\gamma)^{94}\text{Nb}^g$  reaction have been determined to be  $\sigma = 0.18(8)\text{b}$  and  $I = 5.2(8)\text{b}$ , the relatively large uncertainty reflecting that of the  $\beta$  branching ratio of the isomer. While the resonance integral to form the ground state is nearly equal to that for the isomeric state, the thermal cross section of the ground state is much smaller than that of the isomer. The values of these cross sections can be interpreted based on a consideration of the reaction channels that include  $s$ - and  $p$ -wave capture to the resonance states and their subsequent

$\gamma$  decays. This interpretation leads to a comparison with the similar radiative capture by  $^{59}\text{Co}$  and  $^{165}\text{Ho}$ , in which (as also for  $^{93}\text{Nb}$ ) the resonance states can decay to the ground state and isomer through chains with equal numbers of dipole  $\gamma$  rays.

More precise values of the energies and intensities of the  $\gamma$  rays emitted in the decays of  $^{94}\text{Nb}^{g,m}$  and  $^{92}\text{Nb}^m$  have been determined, and correspondingly revised values have been deduced for energy levels in the  $^{94}\text{Mo}$  and  $^{92}\text{Zr}$  daughters.

## ACKNOWLEDGMENTS

The support of the Oregon State University Radiation Center and the assistance of its staff in enabling the reactor irradiations to be carried out are acknowledged with appreciation.

- 
- [1] F. De Corte and A. Simonits, *J. Radioanal. Nucl. Chem.* **133**, 43 (1989).
- [2] T. B. Ryves, *J. Nucl. Energy* **25**, 129 (1971).
- [3] L. Sage and A. K. Furr, *Trans. Am. Nucl. Soc.* **23**, 501 (1976).
- [4] A. Simonits, F. de Corte, E. El Nimr, L. Moens, and J. Hoste, *J. Radioanal. Nucl. Chem.* **81**, 397 (1984).
- [5] F. Farina Arbocò, P. Vermaercke, K. Smits, L. Sneyers, and K. Strijckmans, *J. Radioanal. Nucl. Chem.* **296**, 931 (2013).
- [6] S. F. Mughabghab, *Atlas of Neutron Resonances*, 5th ed. (Elsevier, Amsterdam, 2006).
- [7] <http://www.ortec-online.com/Solutions/applications-software.aspx>.
- [8] P. A. Aarnio, J. T. Routti, and J. V. Sandberg, *J. Radioanal. Nucl. Chem.* **124**, 457 (1988).
- [9] D. Abriola and A. A. Sonzogni, *Nucl. Data Sheets* **107**, 2423 (2006).
- [10] G. Z. He, S. Jiang, Z. Y. Zhou, M. He, W. Z. Tian, J. L. Zhang, L. J. Diao, and H. Li, *Phys. Rev. C* **86**, 014605 (2012).
- [11] S. Hayashibe, N. Yoshikawa, Y. Endo, M. Kanazawa, and T. Ishimatsu, *J. Phys. Soc. Jpn.* **31**, 967 (1971).
- [12] R. G. Helmer, R. C. Greenwood, and R. J. Gehrke, *Nucl. Instrum. Methods* **96**, 173 (1971).
- [13] B. L. Berman and R. J. Baglan, *J. Inorg. Nucl. Chem.* **31**, 9 (1969).
- [14] C. M. Baglin, *Nucl. Data Sheets* **113**, 2187 (2012).
- [15] B. Buck and F. Perey, *Phys. Rev. Lett.* **8**, 444 (1962).
- [16] D. Kompe, *Nucl. Phys. A* **133**, 513 (1969).
- [17] N. J. Drindak *et al.*, *Nucl. Sci. Eng.* **154**, 294 (2006).
- [18] T. Wang, G. Kim, M.-W. Lee, K.-S. Kim, M.-H. Cho, H.-S. Kang, and W. Namkung, *J. Radioanal. Nucl. Chem.* **289**, 945 (2011).
- [19] T. J. Kennett, W. V. Prestwich, and J. S. Tsai, *Can. J. Phys.* **66**, 947 (1988).
- [20] R. E. Chrien, K. Rimawi, and J. B. Garg, *Phys. Rev. C* **3**, 2054 (1971).
- [21] J. R. Huijzena and R. Vandenbosch, *Phys. Rev.* **120**, 1305 (1960).
- [22] R. B. Firestone, S. F. Mughabghab, and G. L. Molnár, *Database of Prompt Gamma Rays from Slow Neutron Capture for Elemental Analysis* (IAEA, Vienna, 2007), Chap. 5.